Available online at www.sciencedirect.com
SCIENCE DIRECT
Journal of Power Sources 150 (2005) 216–222
JOURNAL OF POWER SOURCES
www.elsevier.com/locate/jpowsour

Preparation of co-doped spherical spinel $LiMn_2O_4$ cathode materials for Li-ion batteries

Xiangming He *, Jianjun Li, Yan Cai, Yaowu Wang, Jierong Ying, Changyin Jiang, Chunrong Wan

Materials Chemistry Laboratory, INET, Tsinghua University, P.O. Box 1021, Beijing 102201, PR China

Received 13 August 2004; received in revised form 31 January 2005; accepted 24 February 2005
Available online 2 April 2005

Abstract

Surface cobalt doping and bulk yttrium doping were combined to improve the cycling stability of spherical spinel $LiMn_2O_4$ at elevated temperature (55 °C). The cobalt surface doping was more effective than cobalt bulk doping at the same doping level, because the surface cobalt doping prevents more efficiently manganese from dissolving in electrolyte. At yttrium doping level of 5%, doped spinel $LiMn_2O_4$ had specific capacity in excess of 130 mAh g^{-1} and 120 mAh g^{-1} at first cycle and at 100th cycle, respectively, at 25 °C. Doping of yttrium enhanced the activity of manganese in spinel $LiMn_2O_4$, leading to both increase of specific capacity and decrease of cycleability, because the active manganese easily dissolved into electrolyte during cycling. Moreover, the raise of the temperature led to an intensive dissolution of manganese and poor performance at elevated temperature when yttrium doped. The dissolution could be effectively inhibited by cobalt surface doping. 0.5% yttrium bulk and 0.5% cobalt surface co-doped spherical spinel $LiMn_2O_4$ had the excellent performance, and its initial specific capacities are 118 mAh g^{-1} and 110 mAh g^{-1} at 25 °C and 55 °C, respectively, and its 50th cycle specific capacities remained to be 114 mAh g^{-1} and 91 mAh g^{-1} at 25 °C and 55 °C, respectively.

Keywords: Spherical spinel $LiMn_2O_4$; Co-doping; Yttrium; Cobalt; Elevated temperature

1. Introduction

The past decades have witnessed the rapid development of lithium-ion battery in response to growing the needs from electronic and information industries. Spinel $LiMn_2O_4$ cathode material of Li-ion battery that is cost-effective and environmentally benign, as compared with conventional $LiCoO_2$ material, has been extensively investigated [1–9]. However, instability of spinel $LiMn_2O_4$ during cycling hinders it from practical use. It is deemed that cycling capacity fading is led by dissolution of manganese and structural change [10–12], and that these demerits of spinel $LiMn_2O_4$ can be restrained by doping [13–15]. Among transition metals, cobalt doping is considered to be the most effective. Radius of Co^{3+} is similar to that of Mn^{3+}, and bond energy of Co–O is bigger than that of Mn–O. Substitution of manganese by cobalt can reduce dissolution of manganese in electrolyte, stabilize the lattice of spinel $LiMn_2O_4$, restrain structural change of $LiMn_2O_4$ during cycling, and finally improve its cycleability. But meanwhile the transition metal substitution of manganese decreases specific capacity of spinel $LiMn_2O_4$ [16]. Doping of yttrium can electrochemically activate spinel $LiMn_2O_4$ and increase its specific capacity [17]. But it is found that this activation can also promote dissolution of manganese and worsen its cycleability at 55 °C. Demerit of specific capacity loss by transition metal doping can be overcomes by suitable doping of yttrium, and demerit of poor cycleability by yttrium doping can be overcomes by cobalt surface doping.

The spherical particle could lead to its integrative surface modification to enhance its performance [18]. Our lab has

* Corresponding author. Tel.: +86 10 89796073; fax: +86 10 69771464.
E-mail address: hexm@tsinghua.edu.cn (X. He).

0378-7753/$ – see front matter © 2005 Elsevier B.V. All rights reserved.
doi:10.1016/j.jpowsour.2005.02.029

been engaged in developing spherical active materials for batteries since 1995 [19–22], and developing a process of controlled crystallization to prepare them.

In this study, the spherical spinel $LiMn_2O_4$ powders were prepared. Surface and bulk cobalt doping were carried out to investigate effectiveness of different doping. Doping amount of yttrium was investigated to find out suitable yttrium doping. It was found that yttrium doping promotes the dissolution of manganese in electrolyte, and verified by dissolving tests. Both bulk yttrium doping to improve specific capacity and surface cobalt doping to improve cycleability were carried out to enhance the performance of spherical spinel $LiMn_2O_4$ at elevated temperature (55 °C).

2. Experimental

The preparation of spherical spinel $LiMn_2O_4$ was described in previous report [23]. A brief description is given out as follows.

The spherical $MnCO_3$ was firstly synthesized by controlled crystallization of $MnSO_4{\cdot}H_2O$, NH_4HCO_3 and $NH_3{\cdot}H_2O$. The spherical Mn_2O_3 precursor was then obtained by heat treatment of $MnCO_3$. A mixture of Mn_2O_3 and Li_2CO_3 was calcined to produce $LiMn_2O_4$.

The bulk doping was carried out by co-precipitation with dopant and $MnCO_3$. The cobalt and yttrium bulk doped spinel $LiMn_2O_4$ were prepared from their doped $MnCO_3$, which were co-precipitates of $CoCO_3$ and $MnCO_3$, $Y_2(CO_3)_3$ and $MnCO_3$, and were co-precipitated with NH_4HCO_3 from $MnSO_4$ and $CoSO_4$ solutions, $MnSO_4$ and YCl_3 solutions, respectively. Above mixture solutions were prepared according to desired doping amount. The doped $MnCO_3$ were heated for 4 h at 560 °C and bulk doped Mn_2O_3 were obtained.

The cobalt surface doping was carried out as follows. The obtained Mn_2O_3 was added into deionized water and agitated to form suspension. $CoSO_4$ solution was fed into agitating suspension, meanwhile LiOH solution was also fed slowly into the agitating suspension, according to $[Co^{2+}]/[OH^-] = 1/2$. Thus, $Co(OH)_2$ was coated on the surface of Mn_2O_3.

The obtained Mn_2O_3 was sintered with Li_2CO_3 to prepare desired spinel $LiMn_2O_4$ by the same heating program as described in reference [23].

Manganese dissolution test was carried out by immersion of doped $LiMn_2O_4$ powders in electrolyte of 1 M $LiPF_6$ in EC + DEC (1:1, v/v) for 72 h under the protection of argon. Manganese in electrolyte was analyzed by ICP.

Crystal phase of powders were characterized by powder X-ray diffraction (XRD, D/max-rB) using Cu Kα, 40 kV × 120 mA radiation with step of 0.02° at 6° min^{-1}. The particle morphology of the powders was observed using a scanning electron microscopy (SEM, JSM6301F). The element composition of particle surface was analyzed by EDS (Oxford ATW Link Isis300, resolution 128 eV). Dissolving manganese was detected by ICP-AES (Prodigy, Leeman LABS, Inc.).

The electrode formulation consisted of 80 wt.% $LiMn_2O_4$, 10 wt.% carbon black and 10 wt.% binder. The net load of the doped or un-doped $LiMn_2O_4$ was about 10 mg cm^{-2}. The prepared electrode pellets were dried at 120 °C under vacuum for 48 h. The test coin cells were assembled in a dry glove box filled with argon. The separator was a Celguard 2400 microporous polypropylene membrane. The electrolyte was 1 M $LiPF_6$ in EC + DEC (1:1, v/v). A lithium metal anode was used in this study. The charge/discharge cycling was galvanostatically performed at a current of 0.5 mA cm^{-2} with cut-off voltages of 3.35–4.35 V at room temperature and with cut-off voltage of 3.35–4.2 V at 55 °C.

In this study, percentage of cation or anion is a mole percentage for total cation or total anion, respectively, and is an average percentage corresponding to that introduced during the preparation. Due to the difference of performance between bulk and surface doping, formulation $Li(Mn_{1-x}M_x)_2O_4$ (M = Co and Y) could not correctly represent the samples and was not adopted here. The terminology of surface doping was adopted instead of coating because dopant did diffuse into the bulk at a certain extent during sintering, forming difference of composition between center and outer layer of particles. It is actually partial bulk doping in the outer part of the particles. This was verified by EDS analysis on the surface of particles, indicating that the percentage of dopant on the surface was much higher than the average percentage introduced during the preparation, and by XRD analysis of particles, where the change of intensity and width of reflection peaks indicated that the dopant was located at the sites of spinel crystal, not adhered to the surface of particles, so it was not a coating. Therefore, the term of surface doping was adopted to refer to partial bulk doping in the outer part of the particles.

3. Results and discussion

3.1. Doping of cobalt

All obtained samples are of excellent spherical morphology, fluidity and dispersivity, which are very useful for further processing. The particle diameters are approximate 20 μm. Their SEM images are shown in Figs. 1–3.

The surface morphology of 1% cobalt bulk doped $MnCO_3$ is shown in Fig. 1a. The particle is compactly made up of a number of crystalline grains, which are sized as 1–5 μm. Its surface becomes rough when heated at 560 °C, as shown in Fig. 1b. The roughness is probably caused by emission of CO_2.

Fig. 2 shows the morphology of coated and un-coated Mn_2O_3 by $Co(OH)_2$. The surface of coated Mn_2O_3 becomes rougher, and is closely and uniformly packed by nubby crystalline grains of $Co(OH)_2$, as shown in Fig. 2b. During the

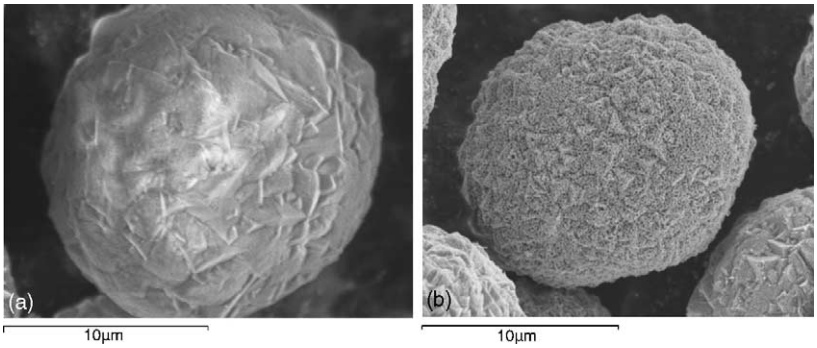

Fig. 1. SEM images of: (a) 1% cobalt bulk doped $MnCO_3$ and (b) 1% cobalt bulk doped Mn_2O_3.

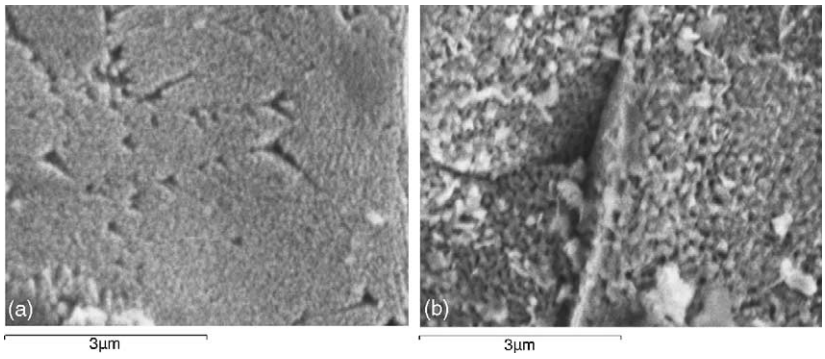

Fig. 2. SEM images of: (a) surface of Mn_2O_3 and (b) $Co(OH)_2$ coated Mn_2O_3.

heat treatment, Co^{2+} ions diffuse into the surface layer of particles to form a cobalt-rich layer of spinel.

Fig. 3 shows the morphology of cobalt doped $LiMn_2O_4$ powders. A distinct difference can be observed between cobalt surface and bulk doped samples, as shown in Fig. 3b and d. The EDS analysis on the surface of 1% cobalt surface doped $LiMn_2O_4$ shows that cobalt percentage was much more than 1% on the surface of doped $LiMn_2O_4$, as shown in

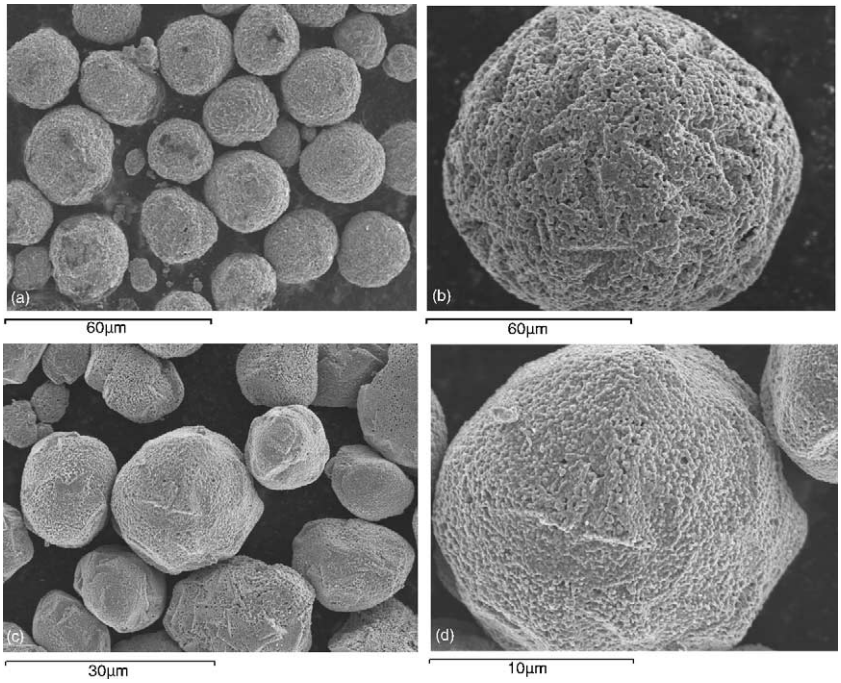

Fig. 3. SEM images of: (a and b) 1% cobalt bulk doped $LiMn_2O_4$ and (c and d) 1% cobalt surface doped $LiMn_2O_4$.

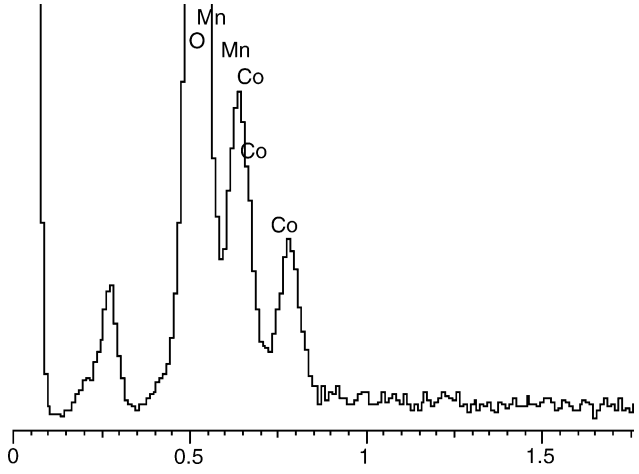

Fig. 4. EDS of 1% cobalt surface doped $LiMn_2O_4$.

Fig. 4. Thereby, surface doping of cobalt can be confirmed to be different from bulk homogeneous doping. For the surface doping samples, doping level is higher in the outer part of particles than that in the central part.

As shown in Fig. 5, XRD patterns of powders show that all cobalt doped $LiMn_2O_4$ are well crystallized and can be identified as pure spinel cubic phases with a space group Fd3m where Li^+ ions occupy the tetrahedral (8a) sites; Mn^{3+}, Mn^{4+} and Co^{3+} ions settle at the octahedral (16d) sites, this is reason why the lattice parameter decreases when cobalt doped; O^{2-} ions reside at (32e). The absence of any other peaks for the XRD patterns of doped spinel $LiMn_2O_4$ samples indicates there are no else phases in the obtained doped samples as compared with pure spinel $LiMn_2O_4$.

There is a very small difference of XRD patterns between 1% cobalt surface doped and 1% cobalt bulk doped samples. This difference causes a very small change of their lattice parameters, as shown in Table 1, and this change indicates that the dopant is homogeneously located in the crystal for bulk doped sample, but not in the surface doped sample, because of their same doping amount. On the other hand, the doping

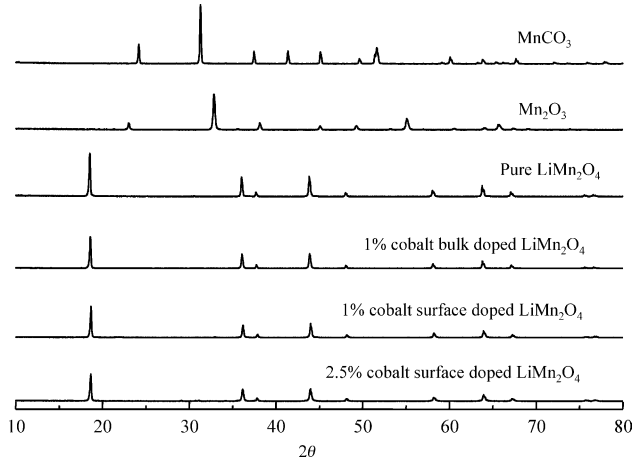

Fig. 5. XRD of cobalt doped $LiMn_2O_4$ and its precursors.

Table 1
Lattice parameters of Co doped $LiMn_2O_4$ (Å)

Pure $LiMn_2O_4$	8.2517
1% Co bulk doped $LiMn_2O_4$	8.2380
1% Co surface doped $LiMn_2O_4$	8.2340
2.5% Co surface doped $LiMn_2O_4$	8.2213

amount is only 1%, it is small and can only make a small impact on XRD patterns of the spinel $LiMn_2O_4$. Hereby, terminology of surface doping is adopted instead of coating in this study.

The radii of Co^{3+} ion (0.063 nm) is smaller than that of Mn^{3+} ion (0.066 nm) and bond energy of Co–O (1067 kJ mole^{-1}) is bigger than that of Mn–O (946 kJ mole^{-1}). The lattice parameter becomes smaller when Co^{3+} ions take the place of Mn^{3+} ions at the octahedral (16d) sites. The lattice parameters of cobalt doped spinel $LiMn_2O_4$ are calculated from the diffraction data and listed in Table 1. Those of cobalt surface doped samples are the smallest. Smaller lattice parameter implies smaller structural change and more stability during cycling. Especially, 1% cobalt surface doped sample has smaller lattice parameter than 1% cobalt bulk doped sample, indicating that it has more stability during cycling. These analyses accord with the cycling performance data. Cobalt surface doped $LiMn_2O_4$ sample has better cycleability.

The cobalt doping causes a loss of initial specific capacity of spinel $LiMn_2O_4$ at room temperature as shown in Fig. 6a. This loss is partially caused by decrease of manganese. The lithium intercalation process should be supported by concomitance of manganese redox. The cobalt substituted for manganese at (16d) sites makes decrease of manganese to participate in redox. In addition, the XRD intensity peaks of the spinel decrease after doping of cobalt, indicating that the crystallinity of spinel $LiMn_2O_4$ and disordering of crystal increase. During discharge, lithium ions intercalate orderly to occupy the tetrahedral (8a) sites at first at voltage plateau of

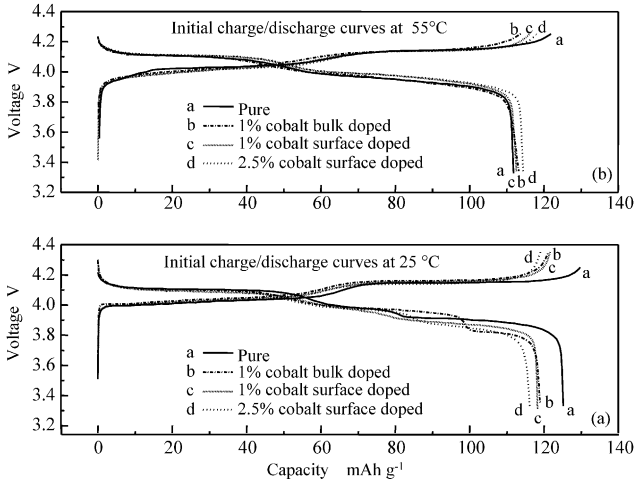

Fig. 6. Initial charge/discharge plateau of cobalt doped $LiMn_2O_4$ at: (a) 25 °C and (b) 55 °C.

4.1 V, and then disorderly fill in at voltage plateau of 3.9 V. The capacity at 4.1 V plateau decreases after cobalt doping (as shown in Fig. 6a). Therefore, increase of crystal disordering causes a loss of specific capacity.

However, the doping restrains the loss of initial specific capacity at elevated temperature (55 °C), as shown in Fig. 6b. The initial specific capacity differences between 25 °C and 55 °C are 13 mAh g^{-1} for pure $LiMn_2O_4$, 7 mAh g^{-1} for 1% cobalt bulk doped sample, 5 mAh g^{-1} for 1% cobalt surface doped sample and 1 mAh g^{-1} for 2.5% cobalt surface doped sample. The most loss happens to pure $LiMn_2O_4$ and the fewest loss happens to the surface doped sample. All initial specific capacities of cobalt doped samples exceed that of pure spinel $LiMn_2O_4$ at 55 °C and the sample of 2.5% cobalt surface doping has the biggest initial specific capacity at 55 °C.

It is considered that the dissolution of manganese in electrolyte is the main reason to cause capacity loss of spinel $LiMn_2O_4$. This dissolution becomes faster at 55 °C than that at 25 °C [10]. Dissolution of manganese in electrolyte can be effectively restrained by cobalt doping, especially surface doping. Consequently, cobalt surface doping can improve capacity of spinel $LiMn_2O_4$ at 55 °C.

The cycling performances of cobalt doped spinel $LiMn_2O_4$ are shown in Fig. 7. Obviously, the cycling performances of spinel $LiMn_2O_4$ can be improved by cobalt doping both at 25 °C and 55 °C, and surface doping is better than bulk doping at the same doping level. One percent cobalt surface doped spherical spinel $LiMn_2O_4$ has synthetically excellent performance for its capacity and cycleability both at 25 °C and 55 °C. At 25 °C, its initial specific capacity is 118 mAh g^{-1} and gets only 9 mAh g^{-1} of capacity loss at 100th cycle, and its initial specific capacity is 113 mAh g^{-1} and remains 93 mAh g^{-1} with capacity retention of 83% at 50th cycle at 55 °C.

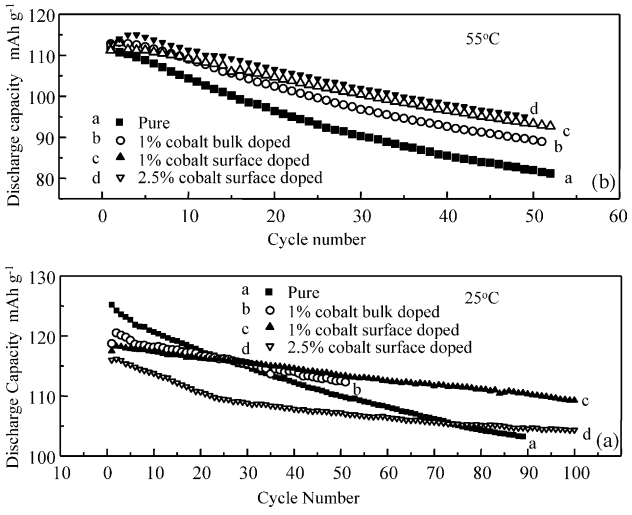

Fig. 7. Cycling performance of cobalt doped $LiMn_2O_4$ at: (a) 25 °C and (b) 55 °C.

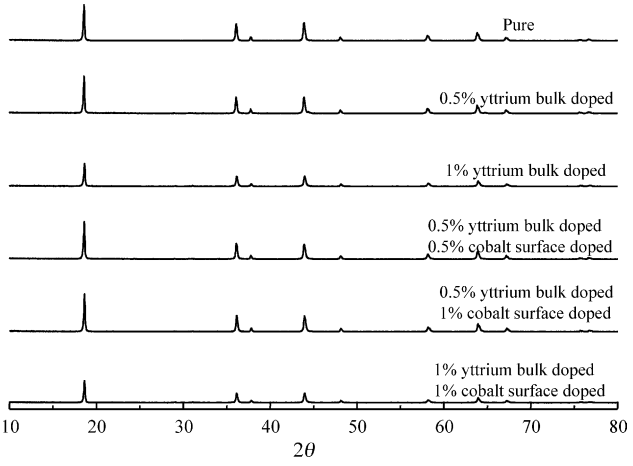

Fig. 8. XRD of cobalt and yttrium doped $LiMn_2O_4$.

Manganese can be effectively restrained to contact with electrolyte by cobalt surface doping, and sequentially prevented from dissolving in electrolyte during cycling. Especially, this prevention is more effective at elevated temperature.

3.2. Co-doping of yttrium and cobalt

As-obtained yttrium doped spherical spinel $LiMn_2O_4$ samples are also of spherality, the same excellent fluidity and dispersivity as cobalt doped samples, and their morphologies are also very similar to that of cobalt doped samples. So their SEM images are not presented here.

As shown in Fig. 8, all the yttrium doped $LiMn_2O_4$ are also well crystallized and identified as pure spinel cubic phases with the same crystal cell structure as the only cobalt doped sample. Yttrium ion takes the place of manganese ion at the octahedral (16d) sites. The lattice parameters of yttrium and cobalt doped spinel $LiMn_2O_4$ are calculated from the diffraction data and listed in Table 2. The lattice parameter of $LiMn_2O_4$ becomes smaller when yttrium doped, but change is tiny. When yttrium doped, the bond energy increases because of excess of formation enthalpy of Y^{3+}–O^{2-} (1905.3 kJ) over that of Mn^{3+}–O^{2-} (959 kJ), and the crystal lattice shrinks. But this shrinkage is limited because of the excess of radii of Y^{3+} (0.088 nm) over that of Mn^{3+} (0.066 nm). Those make structure stable during cycling and are beneficial to improve cycleability.

As shown in Fig. 9, initial specific capacity of 0.5% yttrium doped spinel $LiMn_2O_4$ increases to 130 mAh g^{-1} from 125 mAh g^{-1} at 25 °C and to 120 mAh g^{-1} from

Table 2
Lattice parameters of Y doped $LiMn_2O_4$ (Å)

0.5% Y bulk doped	8.2514
1% Y bulk doped	8.2508
0.5% Co surface and 0.5% Y bulk doped	8.2416
1% Co surface and 0.5% Y bulk doped	8.2388
1% Co surface and 1% Y bulk doped	8.2353

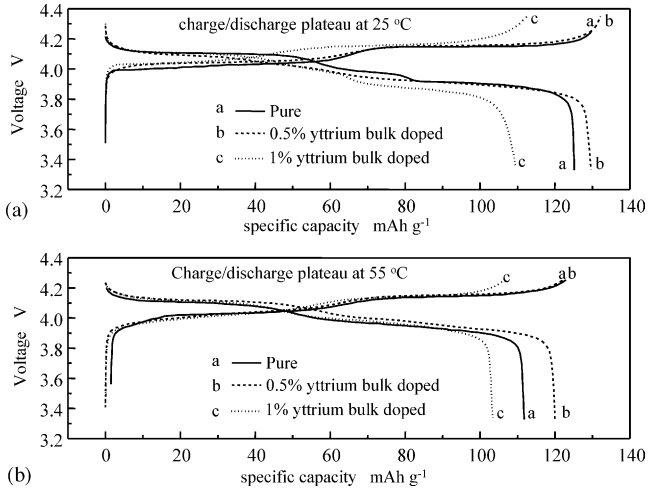

Fig. 9. Initial charge/discharge plateau of cobalt and yttrium doped $LiMn_2O_4$ at: (a) 25 °C and (b) 55 °C.

112 mAh g^{-1} at 55 °C, as compared with pure spinel $LiMn_2O_4$. But that of 1% yttrium doped decreases to 110 mAh g^{-1} at 25 °C and to 103 mAh g^{-1} at 55 °C. Cycling performance also shows the similar effect of yttrium doping. As shown in Fig. 10a, cycleability of 0.5% yttrium doped sample is much better than that of 1% yttrium doped.

The cycling performances of yttrium doped spinel $LiMn_2O_4$ are shown in Fig. 10. Obviously, cycleabilities of 0.5% yttrium doped sample are improved both at 25 °C and 55 °C and its capacity retention is 92.3% at 100th cycle at

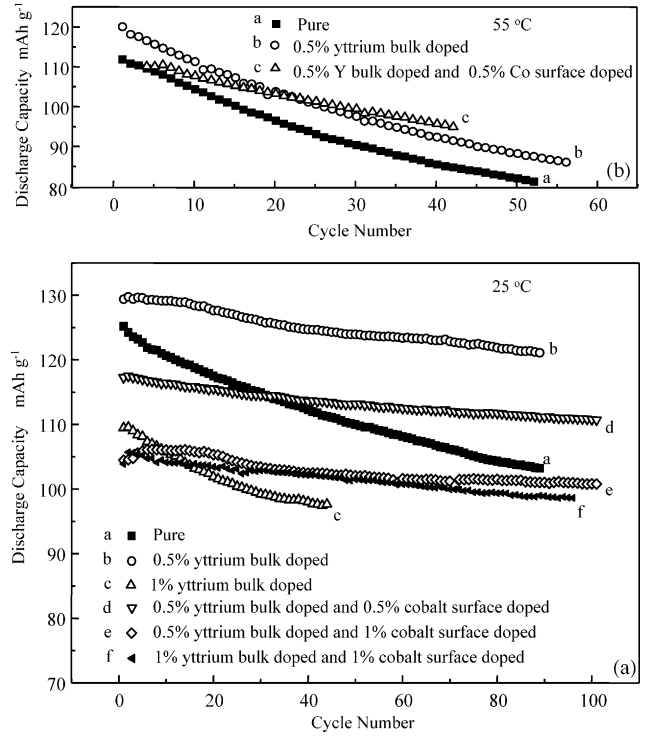

Fig. 10. Cycling performance of yttrium and cobalt doped $LiMn_2O_4$ at: (a) 25 °C and (b) 55 °C.

Table 3
Dissolution of Mn in electrolyte at 25 °C

$LiMn_2O_4$	Dissolution of Mn (%)
Pure	1.16
0.5% Y bulk doped	3.28
1% Y bulk doped	7.03
1% Y bulk and 1% Co surface doped	0.82

25 °C. But at 55 °C, the cycleability is still poor. This is probably caused by intensive dissolution of manganese, which is activated by yttrium, in electrolyte at 55 °C. One percent yttrium doped sample has poor cycleability both at 25 °C and 55 °C. It is noticed that above results are much different from that of other metal doped samples.

In this study, it is found that more yttrium doping leads to more capacity loss and worse cycleability when doping amount exceeds 0.5%, and that 0.5% yttrium doped sample presents higher capacity and better cycleability than those of both un-doped and over 0.5% yttrium doped samples at 25 °C. The doping effect of yttrium is sensitive for electrochemical performance of spinel $LiMn_2O_4$.

Normally, yttrium present in the (16d) site where manganese occupies. Accordingly, the doping of yttrium decreases the content of manganese(3+) in the spinel, and it would lead to a reduction of the capacity. But 0.5% yttrium doped sample has shown the increase capacity as compared with un-doped sample. The reason is probably as follows.

Yttrium is considered to have special catalysis as one of rare earths. In order to explain this special phenomenon, tests of manganese dissolution in electrolyte were carried out and the results are given in Table 3. Obviously, dissolution of manganese increases rapidly as doping amount increases. It concludes that yttrium can significantly activate the manganese in the spinel, leading to an increase of manganese activity. Consequently, yttrium not only activates the electrochemical performance of manganese and enhances the specific capacity of spinel $LiMn_2O_4$, but also promotes the dissolution of manganese in electrolyte and worsens its electrochemical performance. This is why excess yttrium doping causes capacity loss and cycleability worsening. While yttrium doping amount is below 0.5%, doping effect on dissolution of manganese is at acceptable level which is just over that of pure spinel $LiMn_2O_4$, and represents to induce the electrochemical activation of manganese and increase capacity. But effect of more than 0.5% yttrium doping amount on dissolution of manganese surpasses its effect on electrochemical activation of manganese, leading to a worse electrochemical performance. Therefore, only proper yttrium doping can improve the overall electrochemical performance.

Preventing manganese from dissolution in electrolyte and restraining the demerit of yttrium doping, cobalt surface doping is adopted to improve the electrochemical performance of yttrium doped spinel $LiMn_2O_4$.

As shown in Table 3, cobalt surface doping can markedly decrease dissolution of manganese in electrolyte. Meanwhile, cobalt surface doping makes lattice parameter further de-

crease, as shown in Table 2. Because smaller lattice parameter leads to more stable cycling, cobalt surface doping can improve cycleability. Therefore, yttrium bulk and cobalt surface co-doping could enhance the electrochemical performance of spinel $LiMn_2O_4$.

The cycling performances of doped samples are shown in Fig. 10, where 0.5% yttrium bulk and 0.5% cobalt surface co-doped sample has the best cycling performance both at 25 °C and 55 °C, and its specific capacity remains to be 111 mAh g^{-1} and 91 mAh g^{-1}, and capacity retention is 94.2% and 82.7% at 100th cycle at 25 °C and at 50th cycle at 55 °C, respectively. Other samples have either lower capacity or poorer cycleability.

Yttrium bulk and cobalt surface co-doping is an effective way to improve spherical spinel $LiMn_2O_4$ both at 25 °C and 55 °C.

4. Conclusions

The initial specific capacity of $LiMn_2O_4$ decreases when doped with cobalt at 25 °C, but it increases at 55 °C, as compared with un-doped one. The surface cobalt doping is more effective to improve the performance of $LiMn_2O_4$ than bulk cobalt doping at the same doping level. One percent cobalt surface doped sample has overall excellent performance for its capacity and cycleability both at 25 °C and 55 °C. Its initial specific capacity is 118 mAh g^{-1} and gets only 9 mAh g^{-1} of capacity loss at 100th cycle at 25 °C, and it is 113 mAh g^{-1} and remains 93 mAh g^{-1} with capacity retention of 83% at 50th cycle at 55 °C.

The doping of yttrium can electrochemically activate manganese to increase specific capacity of $LiMn_2O_4$; on the other hand, it promotes dissolution of manganese into electrolyte to worsen the performance. 0.5% is a proper amount for yttrium doping. The yttrium bulk and cobalt surface co-doping is an effective way to improve the performance of spherical spinel $LiMn_2O_4$ both at 25 °C and at 55 °C. 0.5% yttrium bulk and 0.5% cobalt surface co-doped sample presents the excellent performance, and its specific capacity remains to be 111 mAh g^{-1} and 91 mAh g^{-1}, and capacity retention is 94.2% and 82.7% at 100th cycle at 25 °C and at 50th cycle at 55 °C, respectively.

References

[1] A. Blyr, C. Sigala, G.G. Amatucci, Y. Chabre, J.M. Tarascon, J. Electrochem. Soc. 145 (1998) 194.
[2] Y. Xia, T. Sakai, T. Fujieda, X.Q. Yang, X. Sun, Z.F. Ma, J. McBreen, J. Electrochem. Soc. 148 (2001) 723A.
[3] G.G. Amatucci, C.N. Schmutz, A. Blyr, C. Sigala, A.S. Gozdz, D. Larcher, J.M. Tarascon, J. Power Sources 69 (1997) 11.
[4] M.M. Thackeray, Y. Shao-Horn, A.J. Kahaian, K.D. Kepler, Electrochem. Solid State Lett. 1 (1998) 7.
[5] J.M. Tarascon, F. Coowar, G. Amatucci, F.K. Shokoohi, D. Guyomard, J. Electrochem. Soc. 141 (1994) 1421.
[6] H. Huang, C.A. Vincent, P.G. Bruce, J. Electrochem. Soc. 146 (1999) 3649.
[7] S.-C. Park, Y.-M. Kim, Y.-M. Kang, K.-T. Kim, P.S. Lee, J.-Y. Lee, J. Power Sources 103 (2001) 86.
[8] S. Park, Y. Han, Y. Kang, P.S. Lee, S. Ahn, H. Lee, J. Lee, J. Electrochem. Soc. 148 (2001) 680.
[9] Z. Li, H. Wang, L. Fang, J.Y. Lee, L.M. Gan, J. Power Sources 104 (2002) 101.
[10] Y.Y. Xia, Y.H. Zhou, M. Yoshio, J. Electrochem. Soc. 144 (1997) 2593.
[11] G.G. Amatucci, N. Pereira, T. Zheng, J.-M. Tarascon, J. Electrochem. Soc. 148 (2001) A171.
[12] J. Choa, M.M. Thackeray, J. Electrochem. Soc. 146 (1999) 3577.
[13] H.C. Wang, C.H. Lu, J. Power Sources 119–121 (2003) 738.
[14] C. Vogler, A. Butz, H. Dittrich, G. Arnold, M. Wohlfahrt-Mehrens, J. Power Sources 84 (1999) 243.
[15] J.M. Amarilla, J.L. Martýn de Vidales, R.M. Rojas, Solid State Ionics 127 (2000) 73.
[16] H.S. Moon, J.W. Park, J. Power Sources 119–121 (2003) 717.
[17] C.Q. Feng, H. Tang, K.L. Zhang, J.T. Sun, Mater. Chem. Phys. 80 (2003) 573.
[18] X.H. Du, C.Y. Jiang, C.R. Wan, J. Tsinghua Univ. (Sci. Technol.) 41 (2001) 71.
[19] C.Y. Jiang, C.R. Wan, Q.R. Zhang, J.J. Zhang, Chin. J. Power Sources 21 (1997) 243.
[20] C.Y. Jiang, Q.R. Zhang, X.H. Du, C.R. Wan, Chin. J. Power Sources 24 (2000) 207.
[21] J.R. Ying, C.Y. Jiang, C.R. Wan, J. Power Sources 129 (2004) 264.
[22] J.R. Ying, C.Y. Jiang, C.R. Wan, J. Power Sources 99 (2001) 78.
[23] X.M. He, J.J. Li, Y. Cai, Y.W Wang, J.R. Ying, C.Y Jiang, C.R. Wan, J. Solid State Electrochem, 15 December, 2004, press online, http://springer.metapress.com.